Republic of Iraq
Ministry of Higher Education
and Scientific Research
University of Diyala
College of Science

Structural, Electrical and Optical Properties of Synthesized Perovskite NPs/PVDF nanocomposites

A Thesis
Submitted to the Council of College of Science
University of Diyala in Partial Fulfillment of Requirements for the
Degree of Doctor of Philosophy (Ph.D.) in Physics

By

Aws Khawwam Mohammed

(B.Sc. in Physics 2011)
(M.Sc. in Physics 2014)

Supervised by

Prof. Dr.
Sabah A. Salman

Prof. Dr.
Farah T. M. Noori

1440 A. H.

2019 A. D.

﴿وَعِنْدَهُ مَفَاتِحُ الْغَيْبِ لَا يَعْلَمُهَا إِلَّاهُو وَيَعْلَمُ مَافِي الْبَرِّ وَالْبَحْرِ وَمَا تَسْقُطُ مِنْ وَرَقَةٍ إِلَّا يَعْلَمُهَا وَلَا حَبَّةٍ فِي ظُلُمَاتِ الْأَرْضِ وَلَا رَطْبٍ وَلَا يَابِسٍ إِلَّا فِي كِتَابٍ مُبِينٍ ﴾

"And with Him are the keys of the unseen; none knows them except Him. And He knows what is on the land and in the sea. Not a leaf falls but that He knows it. And no grain is there within the darknesses of the earth and no moist or dry [thing] but that it is [written] in a clear record".

Surah Al-An'am (59) سورة الانعام الأية

Dedication

To my Family…

AWS

Acknowledgments

First and foremost, I thank Allah (SWT) for letting me live to see this thesis through and gave me chance and courage to complete this work, and our prophet Muhammad (peace and blessings of Allah be upon him) who invites us to science and knowledge.

I would like to express my sincere gratitude to my supervisors Prof. Dr. Sabah A. Salman and Prof. Dr. Farah T. M. Noori who granted me the opportunity to do this research. I am indebted to them for their suggestions and valuable remarks.

Special thank are extended to the Dean of the College of Science and to head of Physics Department Assist. Prof. Dr. Ziad T. Khodair and all the Staff of the Department of Physics for their assistance.

My greatest indebtedness goes to my Parents for their valuable advice, my Brothers (Saif and Ali), my Sisters (Saja and Reham) and my Wife (Ebada) for their endless support.

Finally, my deepest gratitude is dedicated to my Studying Partners: Ahmed, Wisam, Ali and Marwa and especially Haydar Ali who shares every happy and sad moment with me...

Supervisors Certification

We certify that this thesis has been prepared under our supervision at the University of Diyala / College of Sciences / Department of Physics as a partial fulfillment of the requirements for the Degree of doctor of philosophy (Ph.D.) in Physics.

Signature:

Name: **Dr. Sabah A. Salman**

Title: Professor

Date: 16 / 9 / 2018

Signature:

Name: **Dr. Farah T. M. Noori**

Title: Professor

Date: 16 / 9 / 2018

In view of available recommendation, I forward this thesis for debate by the examining committee.

Signature:

Name: **Dr. Jassim M. Mansour**

Title: Lecturer

Head of the Department of Physics

Date: 16 / 9 / 2018

Linguistic Amendment

I certify that the thesis entitled **"Structural, Electrical and Optical Properties of Synthesized Perovskite NPs/PVDF nanocomposites"** presented by (**Aws Khawwam Mohammed**), has been corrected linguistically, therefore, it is suitable for debate be examination committee.

Signature:

Name: **Nizar H. Wali**

Title: Assistant Professor

Address: University of Diyala

Date: 3 / 4 / 2019

Scientific Amendment

I certify that the thesis entitled **"Structural, Electrical and Optical Properties of Synthesized Perovskite NPs/PVDF nanocomposites"** presented by (**Aws Khawwam Mohammed**), has been evaluated scientifically, therefore, it is suitable for debate be examination committee.

Signature:

Name: **Dr. Farouq I. Hussain**

Title: Assistant Professor

Address: University of Baghdad

Date: 25 / 3 / 2019

Examination Committee Certificate

We certify that we have read this thesis entitled " **Structural, Electrical and Optical Properties of Synthesized Perovskite NPs/PVDF nanocomposites**" and, as an examining committee, we examined the student (**Aws Khawwam Mohammed**) on its content and in what is related to it, and that in our opinion it meets the standard of a thesis for the degree of Doctor of Philosophy in Physics.

Signature
Name: **Prof. Dr. Tahseen H. Mubarak**
Address: University of Diyala
Date: 21/2/2019
Chairman

Signature
Name: **Prof. Dr. Nabeel A. Bakr**
Address: University of Diyala
Date: 17/2/2019
Member

Signature
Name: **Assist. Prof. Dr. Bahjat B. kadim**
Address: Al-Mustansiriyah University
Date: 19/2/2019
Member

Signature
Name:**Assist. Prof. Dr. Adnan R. Ahmed**
Address: University of Tikrit
Date: 19/2/2019
Member

Signature
Name: **Assist. Prof. Dr. Zainab J. Shnan**
Address: University of Baghdad
Date: 19/2/2019
Member

Signature
Name: **Prof. Dr. Sabah A. Salman**
Address: University of Diyala
Date: 19/2/2019
Supervisor

Signature
Name: **Prof. Dr. Farah T. M. Noori**
Address: University of Baghdad
Date: 19/2/2019
Supervisor

Approved by the Council of the College of Science.
(The Dean)
Signature:
Name: **Prof. Dr. Tahseen H. Mubarak**
Date: 21/2/2019

Published and Accepted Research Articles

1. S. A. Salman, F. T. Noori and A. K. Mohammed, "Preparation and Characterizations of Poly (vinylidene fluoride) (PVDF)/$Ba_{0.6}Sr_{0.4}TiO_3$ (BST) Nanocomposites", International Journal of Applied Engineering Research, Vol. 13, No. 7, pp. 5008-5013, (2018).
2. F. T. Noori, A. K. Mohammed and S. A. Salman " High energy Gamma Irradiation processing of PVDF/$Ba_xSr_{1-x}TiO_3$ Bio-nanocomposite on Optical Properties", Journal of Chemical, Biological and Physical Sciences, Vol. 9, No. 1, pp. 067-077, (2018).
3. A. K. Mohammed, F. T. Noori, and S. A. Salman "Hydrothermal Synthesis of Nano BST Alloy and Studying The Piezoelectric, Optical Properties of Poly(vinylidenefluoride) (PVDF)/ $Ba_{0.6}Sr_{0.4}TiO_3$ (BST) Nanocomposites", ARPN Journal of Engineering and Applied Sciences, Vol. 14, No. 3, pp. 622-629 (2019).

Abstract

Poly(vinylidene fluoride) (PVDF)/Barium Strontium Titanate $Ba_xSr_{1-x}TiO_3$ (x= 0.6, 0.7) (BST) nanocomposites with different filler contents of (BST) have been fabricated by using solution casting method. The structural, dielectric, optical and piezoelectric properties and the effect of the gamma irradiation with doses (4.32 kGy) and (4.98 kGy) on the optical properties of PVDF/$Ba_xSr_{1-x}TiO_3$ (x= 0.6, 0.7) nanocomposites have been investigated.

The (XRD) results of the $Ba_xSr_{1-x}TiO_3$ (x= 0.6, 0.7) nanopowders obtained by hydrothermal method showed that the (BST6) nanopowder has cubic perovskite structure and (BST7) nanopowder has tetragonal perovskite structure. The crystallite size of PVDF/$Ba_xSr_{1-x}TiO_3$ (x= 0.6, 0.7) nanocomposites was calculated using Scherrer and Williamson-Hall (W-H) equations and it is observed that the crystallite size increases with the increasing of the filler content of (BST).

The frequency dependency of dielectric constant, dielectric losses and AC conductivity of the PVDF/$Ba_xSr_{1-x}TiO_3$ (x= 0.6, 0.7) naocomposites with different filler contents of (BST) in frequency range (50Hz–1MHz) at room temperature were studied. The dielectric constant of the PVDF/ $Ba_xSr_{1-x}TiO_3$ (x= 0.6, 0.7) nanocomposite increases with the increasing of (BST) filler content at the same frequency. The dielectric losses and AC conductivity of the PVDF/$Ba_xSr_{1-x}TiO_3$ (x= 0.6, 0.7) nanocomposites increase with the increasing of (BST) filler content at the same frequency. The dielectric properties of (PVDF) polymer were improved by increasing (BST) filler content.

The optical properties were studied from the absorbance spectrum, the absorbance of the PVDF/$Ba_xSr_{1-x}TiO_3$ (x= 0.6, 0.7) nanocomposites increases with the increasing of (BST) filler content. The optical energy gap for the direct allowed electronic transition of PVDF/$Ba_{0.6}Sr_{0.4}TiO_3$ nanocomposite with different filler contents of (BST) decreases from (3.9 eV) to (3.2 eV) with the increasing of the (BST6) filler content, and the optical energy gap of PVDF/$Ba_{0.7}Sr_{0.3}TiO_3$ nanocomposite with different filler contents of (BST) decreases as the (BST7) filler content increases.

The absorbance of the PVDF/$Ba_xSr_{1-x}TiO_3$ (x= 0.6, 0.7) nanocomposites increases after gamma irradiation with doses (4.32 kGy) and (4.98 kGy). The optical energy gap of the PVDF/$Ba_xSr_{1-x}TiO_3$ (x= 0.6, 0.7) nanocomposites decreases after gamma irradiation with doses (4.32 kGy) and (4.98 kGy).

The results of piezoelectric measurements showed that the resistance of all the PVDF/$Ba_{0.6}Sr_{0.4}TiO_3$ nanocomposites decreases as the applied pressure increases, the resistance of the PVDF/$Ba_{0.6}Sr_{0.4}TiO_3$ nanocomposite increased with the increasing of (BST6) filler content at the same applied pressure. The resistance of PVDF/$Ba_{0.6}Sr_{0.4}TiO_3$ (PVDF/BST6) nanocomposites made with the surface-hydroxylated (PVDF/BST6-OH) is lower than the resistance of (PVDF/BST6) nanocomposites at the same applied pressure.

Contains

	Subject	Page
	Contains	I
	List of Figures	VI
	List of Tables	XIV
	List of Symbols and Abbreviations	XVI
Chapter 1	**Introduction and Previous Studies**	1-24
1.1	Introduction	1
1.2	Polymer composites	3
1.3	Piezoelectric Materials	5
1.4	Piezoelectric Polymers	7
1.4.1	Applications of Piezoelectric Polymers	8
1.5	Poly(vinylidene fluoride) (PVDF)	8
1.6	Ferroelectric Perovskite Materials	12
1.7	Barium Strontium Titanate (BST)	12
1.8	Previous Studies	15
1.9	Aims of the Study	24
Chapter 2	**Theoretical Part**	25–44
2.1	Introduction	25
2.2	Hydrothermal synthesis	25
2.3	Structural Properties	27

	Subject	Page
2.3.1	X-Ray Diffraction (XRD) and Bragg's Law	27
2.3.2	Structural Parameters	30
2.3.2.1	Lattice Constants	30
2.3.2.2	Average Crystallite Size (D)	30
2.4	Dielectric Properties	31
2.4.1	Dielectric Constant	31
2.4.2	Dielectric Loss	32
2.4.3	AC Conductivity	36
2.5	Optical Properties	36
2.5.1	Transmittance (T)	37
2.5.2	Absorbance (A)	37
2.5.3	Absorption coefficient (α)	37
2.5.4	Electronic Transitions	37
2.5.4.1	The Direct Transitions	38
2.5.4.2	The Indirect Transitions	39
2.5.5	Optical Energy Gap (Eg)	41
2.6	Piezoelectric Effect	41
2.7	Effect of Radiation on Materials	43
Chapter 3	**Experimental Part**	45-56
3.1	Introduction	45
3.2	Preparation of Barium Strontium Titanate (BST) Nanopowder	45

	Subject	Page
3.2.1	Materials	45
3.2.2	Method of Preparation of Barium Strontium Titanate (BST) Nanopowder	46
3.2.3	Surface Hydroxylation of Barium Strontium Titanate (BST)	47
3.3	Preparation of (PVDF/BST) Composites	48
3.4	Structural Measurements	49
3.4.1	X-Ray Diffraction (XRD)	49
3.4.2	Atomic Force Microscopy (AFM)	49
3.4.3	Field-Emission Scanning Electron Microscopy (FESEM)	51
3.4.4	Fourier Transform Infrared Spectroscopy (FTIR)	52
3.5	Dielectric Measurements	54
3.5.1	LCR –Meter	54
3.6	Piezoelectric Measurements	55
3.7	Optical Measurements	56
3.8	Samples Irradiation	56
Chapter 4	**Results and Discussion**	57−125
4.1	Introduction	57
4.2	Results of Structural Measurements	57
4.2.1	X-ray Diffraction (XRD)	57
4.2.1.1	$Ba_xSr_{1-x}TiO_3$ (BST) Nanopowders	57
4.2.1.2	Poly(vinylidene fluoride) Polymer Film	61

	Subject	Page
4.2.1.3	PVDF/$Ba_{0.6}Sr_{0.4}TiO_3$ Nanocomposites	64
4.2.1.4	PVDF/ $Ba_{0.7}Sr_{0.3}TiO_3$ Nanocomposites	74
4.2.2	Atomic Force Microscopy (AFM)	79
4.2.3	Field-Emission Scanning Electron Microscopy (FESEM)	81
4.2.4	Fourier Transform Infrared Spectroscopy (FTIR)	86
4.2.4.1	$Ba_xSr_{1-x}TiO_3$ (BST) Nanopowders	86
4.2.4.2	Poly(vinylidene fluoride) (PVDF) Polymer Film	87
4.2.4.3	PVDF/$Ba_{0.6}Sr_{0.4}TiO_3$ Nanocomposites	88
4.2.4.4	PVDF/ $Ba_{0.7}Sr_{0.3}TiO_3$ Nanocomposites	89
4.3	Results of Dielectric Measurements	90
4.3.1	PVDF/$Ba_{0.6}Sr_{0.4}TiO_3$ Nanocomposites	91
4.3.2	PVDF/ $Ba_{0.7}Sr_{0.3}TiO_3$ Nanocomposites	96
4.3.3	Effect of Surface Hydroxylation of Barium Strontium Titanate (BST)	98
4.4	Results of Optical Measurements	104
4.4.1	PVDF/$Ba_{0.6}Sr_{0.4}TiO_3$ Nanocomposites	104
4.4.2	PVDF/$Ba_{0.7}Sr_{0.3}TiO_3$ Nanocomposites	109
4.4.3	Effect of Gamma Irradiation of (PVDF/ $Ba_xSr_{1-x}TiO_3$) Nanocomposites	112
4.4.3.1	PVDF/$Ba_{0.6}Sr_{0.4}TiO_3$ Nanocomposites	112
4.4.3.2	PVDF/$Ba_{0.7}Sr_{0.3}TiO_3$ Nanocomposites	119

	Subject	Page
4.5	Results of Piezoelectric Measurements	124
Chapter 5	**Conclusions and Future Works**	126–128
5.1	Conclusions	126
5.2	Future Works	127
	References	129

List of Figures

No.	Title	Page
Chapter 1	**Introduction and Previous Studies**	1−24
(1-1)	Structure of (PVDF)	9
(1-2)	Schematic representation of the chain formation for the α, β and γ-phases of (PVDF)	11
(1-3)	(a) paraelectric phase (centro-symmetric) (b) ferroelectric phase (displaced) of (BST)	13
(1-4)	BST Curie temperature is linearly dependent on concentration of Sr	14
Chapter 2	**Theoretical Part**	25−44
(2-1)	Schematic representation of Bragg diffraction of x-ray by plans of atoms	28
(2-2)	Schematic diagram of typical components and angles of the gonimeter for a θ-2θ x-ray diffractometer	29
(2-3)	Simplified diagram of currents in a loss dielectric	34
(2-4)	Types of electronic transitions	40
(2-5)	A diagram illustrating the (a) direct and (b) converse piezoelectric effects.	42
Chapter 3	**Experimental Part**	45−56
(3-1)	Autoclave used for hydrothermal synthesis	46
(3-2)	Schematic diagrams of the hydroxylation of (BST) particles and formation of Hydrogen bond in (PVDF/BST) composites	47

No.	Title	Page
(3-3)	A schematic presentation of atomic force microscopy (AFM).	50
(3-4)	Schematic of a field emission scanning electron microscope (FESEM).	52
(3-5)	A Schematic representing (FTIR) spectrophotometer.	54
(3-6)	A Schematic of piezoelectric apparatus.	55
(3-7)	A schematic diagram shows how the UV–visible spectrometer works.	56
Chapter 4	**Results and Discussion**	57−125
(4-1)	(XRD) pattern of the $Ba_{0.6}Sr_{0.4}TiO_3$ nanopowder.	57
(4-2)	(XRD) pattern of the $Ba_{0.7}Sr_{0.3}TiO_3$ nanopowder.	59
(4-3)	Williamson-Hall (W-H) analysis of (a) $Ba_{0.6}Sr_{0.4}TiO_3$ (b) $Ba_{0.7}Sr_{0.3}TiO_3$ nanopowders.	60
(4-4)	(XRD) pattern of the (PVDF) polymer film.	62
(4-5)	Williamson-Hall (W-H) analysis of (PVDF) polymer film	63
(4-6)	(XRD) pattern of PVDF/$Ba_{0.6}Sr_{0.4}TiO_3$ nanocomposite with (5vol%) filler content.	65
(4-7)	(XRD) pattern of PVDF/$Ba_{0.6}Sr_{0.4}TiO_3$ nanocomposite with (10vol%) filler content.	65
(4-8)	(XRD) pattern of PVDF/$Ba_{0.6}Sr_{0.4}TiO_3$ nanocomposite with (15vol%) filler content.	66
(4-9)	(XRD) pattern of PVDF/$Ba_{0.6}Sr_{0.4}TiO_3$ nanocomposite with (20vol%) filler content.	66
(4-10)	(XRD) pattern of PVDF/$Ba_{0.6}Sr_{0.4}TiO_3$ nanocomposite with (25vol%) filler content.	68

No.	Title	Page
(4-10)	(XRD) pattern of PVDF/$Ba_{0.6}Sr_{0.4}TiO_3$ nanocomposite with (30vol%) filler content.	69
(4-10)	(XRD) pattern of PVDF/$Ba_{0.6}Sr_{0.4}TiO_3$ nanocomposite with (35vol%) filler content.	69
(4-10)	(XRD) pattern of PVDF/$Ba_{0.6}Sr_{0.4}TiO_3$ nanocomposite with (40vol%) filler content.	71
(4-14)	Williamson-Hall (W-H) analysis of PVDF/$Ba_{0.6}Sr_{0.4}TiO_3$ nanocomposites with (a): 5, (b): 10, (c): 15, (d):20, (e): 25, (f): 30, (g): 35 and (h): 40 vol% filler contents.	72−73
(4-15)	(XRD) pattern of PVDF/$Ba_{0.7}Sr_{0.3}TiO_3$ nanocomposite with (25vol%) filler content.	75
(4-16)	(XRD) pattern of PVDF/$Ba_{0.7}Sr_{0.3}TiO_3$ nanocomposite with (30vol%) filler content.	75
(4-17)	(XRD) pattern of PVDF/$Ba_{0.7}Sr_{0.3}TiO_3$ nanocomposite with (35vol%) filler content.	76
(4-18)	(XRD) pattern of PVDF/$Ba_{0.7}Sr_{0.3}TiO_3$ nanocomposite with (40vol%) filler content.	76
(4-19)	Williamson-Hall (W-H) analysis of PVDF/$Ba_{0.7}Sr_{0.3}TiO_3$ nanocomposites with (a): 25, (b): 30, (c): 35, (d): 40 vol% filler contents.	78
(4-20)	(AFM) of $Ba_{0.6}Sr_{0.4}TiO_3$ nanopowder.	80
(4-21)	(AFM) of $Ba_{0.7}Sr_{0.3}TiO_3$ nanopowder.	80
(4-22)	(FESEM) images of PVDF/$Ba_{0.6}Sr_{0.4}TiO_3$ nanocomposite with (5 vol%) filler content at different magnifications.	82
(4-23)	(FESEM) images of PVDF/$Ba_{0.6}Sr_{0.4}TiO_3$ nanocomposite with (20 vol%) filler content at different magnifications.	83

No.	Title	Page
(4-24)	(FESEM) images of PVDF/$Ba_{0.6}Sr_{0.4}TiO_3$ nanocomposite with (40 vol%) filler content at different magnifications.	84
(4-25)	(FESEM) images of PVDF/$Ba_{0.7}Sr_{0.3}TiO_3$ nanocomposite with (40 vol%) filler content at different magnifications.	85
(4-26)	(FTIR) spectra of the $Ba_{0.6}Sr_{0.4}TiO_3$ (BST6) and (BST6-OH) nanopowders.	86
(4-27)	(FTIR) spectra of the $Ba_{0.7}Sr_{0.3}TiO_3$ (BST7) and (BST7-OH) nanopowders.	87
(4-28)	(FTIR) spectra of (PVDF) polymer film.	88
(4-29)	(FTIR) spectra of PVDF/$Ba_{0.6}Sr_{0.4}TiO_3$ nanocomposites with (5, 15, 25 and 40) vol% filler contents.	89
(4-30)	(FTIR) spectra of PVDF/$Ba_{0.7}Sr_{0.3}TiO_3$ nanocomposites with (25 and 40) vol% filler contents.	90
(4-31)	Dielectric constant as a function of frequency of the PVDF/ $Ba_{0.6}Sr_{0.4}TiO_3$ nanocomposites with (0, 5, 10, 15 and 20) vol% filler contents.	92
(4-32)	Dielectric constant as a function of frequency of the PVDF/ $Ba_{0.6}Sr_{0.4}TiO_3$ nanocomposites with (25, 30, 35 and 40) vol% filler contents.	92
(4-33)	Dielectric losses as a function of frequency of the PVDF/ $Ba_{0.6}Sr_{0.4}TiO_3$ nanocomposites with (0, 5, 10, 15 and 20) vol% filler contents	93
(4-34)	Dielectric losses as a function of frequency of the PVDF/ $Ba_{0.6}Sr_{0.4}TiO_3$ nanocomposites with (25, 30, 35 and 40) vol% filler contents	93

No.	Title	Page
(4-35)	AC conductivity as a function of frequency of the PVDF/ $Ba_{0.6}Sr_{0.4}TiO_3$ nanocomposites with (0, 5, 10, 15 and 20) vol% filler contents.	95
(4-36)	AC conductivity as a function of frequency of the PVDF/ Ba0.6Sr0.4TiO3 nanocomposites with (25, 30, 35 and 40) vol% filler contents.	95
(4-37)	Dielectric constant as a function of frequency of the PVDF/ $Ba_{0.7}Sr_{0.3}TiO_3$ nanocomposites with (25, 30, 35 and 40) vol% filler contents	97
(4-38)	Dielectric losses as a function of frequency of the PVDF/ $Ba_{0.7}Sr_{0.3}TiO_3$ nanocomposites with (25, 30, 35 and 40) vol% filler contents	97
(4-39)	AC conductivity as a function of frequency of the PVDF/ $Ba_{0.7}Sr_{0.3}TiO_3$ nanocomposites with (25, 30, 35 and 40) vol% filler contents	98
(4-40)	Dielectric constant and dielectric losses as a function of frequency of (PVDF/BST6) and (PVDF/BST6-OH) nanocomposites with (5vol%) filler content	99
(4-41)	Dielectric constant and dielectric losses as a function of frequency of (PVDF/BST6) and (PVDF/BST6-OH) nanocomposites with (20vol%) filler content	100
(4-42)	Dielectric constant and dielectric losses as a function of frequency of (PVDF/BST6) and (PVDF/BST6-OH) nanocomposites with (25vol%) filler content	100
(4-43)	Dielectric constant and dielectric losses as a function of frequency of (PVDF/BST6) and (PVDF/BST6-OH) nanocomposites with (35vol%) filler content	101

No.	Title	Page
(4-44)	AC conductivity as a function of frequency of (PVDF/BST6) and (PVDF/BST6-OH) nanocomposites with (5vol%) filler content	102
(4-45)	AC conductivity as a function of frequency of (PVDF/BST6) and (PVDF/BST6-OH) nanocomposites with (20vol%) filler content	102
(4-46)	AC conductivity as a function of frequency of (PVDF/BST6) and (PVDF/BST6-OH) nanocomposites with (25vol%) filler content	103
(4-47)	AC conductivity as a function of frequency of (PVDF/BST6) and (PVDF/BST6-OH) nanocomposites with (35vol%) filler content	103
(4-48)	Absorption spectra of (PVDF/BST6) nanocomposites with (5, 10, 15 and 20) vol% filler contents	105
(4-49)	Absorption spectra of (PVDF/BST6) nanocomposites with (25, 30, 35 and 40) vol% filler contents	105
(4-50)	Optical energy gap of (PVDF/BST6) nanocomposite with (5 vol%) filler content.	107
(4-51)	Optical energy gap of (PVDF/BST6) nanocomposite with (10 vol%) filler content.	107
(4-52)	Optical energy gap of (PVDF/BST6) nanocomposite with (15 vol%) filler content.	107
(4-52)	Optical energy gap of (PVDF/BST6) nanocomposite with (20 vol%) filler content.	107
(4-53)	Optical energy gap of (PVDF/BST6) nanocomposite with (25 vol%) filler content.	108
(4-53)	Optical energy gap of (PVDF/BST6) nanocomposite with (30 vol%) filler content.	108
(4-53)	Optical energy gap of (PVDF/BST6) nanocomposite with (35 vol%) filler content.	108

No.	Title	Page
(4-54)	Optical energy gap of (PVDF/BST6) nanocomposite with (40 vol%) filler content.	108
(4-58)	Absorption spectra of (PVDF/BST7) nanocomposites with (25, 30, 35 and 40) vol% filler contents	109
(4-59)	Optical energy gap of (PVDF/BST7) nanocomposite with (25 vol%) filler content.	111
(4-60)	Optical energy gap of (PVDF/BST7) nanocomposite with (30 vol%) filler content.	111
(4-61)	Optical energy gap of (PVDF/BST7) nanocomposite with (35 vol%) filler content.	111
(4-62)	Optical energy gap of (PVDF/BST7) nanocomposite with (40 vol%) filler content.	111
(4-63)	Absorption spectra of (PVDF/BST6) nanocomposite with (5 vol%) filler content unirradiated and irradiated with doses (4.32 kGy) and (4.98 kGy)	113
(4-64)	Absorption spectra of (PVDF/BST6) nanocomposite with (25vol%) filler content unirradiated and irradiated with doses (4.32 kGy) and (4.98 kGy)	113
(4-65)	Absorption spectra of (PVDF/BST6) nanocomposite with (40 vol%) filler content unirradiated and irradiated with doses (4.32 kGy) and (4.98 kGy)	114
(4-66)	Optical energy gap of (PVDF/BST6) nanocomposite with (5 vol%) filler content (a) unirradiated (b) irradiated (4.32 kGy) (c) irradiated (4.98 kGy)	116
(4-67)	Optical energy gap of (PVDF/BST6) nanocomposite with (25 vol%) filler content (a) unirradiated (b) irradiated (4.32 kGy) (c) irradiated (4.98 kGy)	117

No.	Title	Page
(4-68)	Optical energy gap of (PVDF/BST6) nanocomposite with (40 vol%) filler content (a) unirradiated (b) irradiated (4.32 kGy) (c) irradiated (4.98 kGy)	118
(4-69)	Absorption spectra of (PVDF/BST7) nanocomposite with (25 vol%) filler content unirradiated and irradiated with doses (4.32 kGy) and (4.98 kGy)	120
(4-70)	Absorption spectra of (PVDF/BST7) nanocomposite with (40 vol%) filler content unirradiated and irradiated with doses (4.32 kGy) and (4.98 kGy).	120
(4-71)	Optical energy gap of (PVDF/BST7) nanocomposite with (25 vol%) filler content (a) unirradiated (b) irradiated (4.32 kGy) (c) irradiated (4.98 kGy).	122
(4-72)	Optical energy gap of (PVDF/BST7) nanocomposite with (40 vol%) filler content (a) unirradiated (b) irradiated (4.32 kGy) (c) irradiated (4.98 kGy)	123
(4-73)	The relation between applied pressure and resistance for (PVDF/BST6-OH) nanocomposites with different filler contents	124
(4-74)	The relation between applied pressure and resistance for (PVDF/BST6) nanocomposites with different filler contents	125

List of Tables

No.	Title	Page
Chapter 1	**Introduction and Previous Studies**	1−24
(1-1)	Dielectric constant (ε′) and loss tangent (tanδ) of some polymers	4
Chapter 3	**Experimental Part**	45−56
(3-1)	The characteristics of the materials	45
(3-2)	The weight compounds used for the preparation of BST nanopowder.	46
(3-3)	Volume fractions of (BST) in (PVDF) matrix	49
Chapter 4	**Results and Discussion**	57−125
(4-1)	(JCPDS) card and (XRD) data of $Ba_{0.6}Sr_{0.4}TiO_3$ nanopowder	58
(4-2)	(JCPDS) card and (XRD) data of $Ba_{0.7}Sr_{0.3}TiO_3$ nanopowder.	59
(4-3)	Average crystallite size, microstrain and lattice constants of $Ba_{0.6}Sr_{0.4}TiO_3$ and $Ba_{0.7}Sr_{0.3}TiO_3$ nanopowders.	61
(4-4)	(XRD) data of (PVDF) polymer film	62
(4-5)	Average crystallite size and microstrain of (PVDF) polymer film	63
(4-6)	(XRD) data of PVDF/$Ba_{0.6}Sr_{0.4}TiO_3$ nanocomposites with different filler contents	67
(4-7)	(XRD) data of PVDF/$Ba_{0.6}Sr_{0.4}TiO_3$ nanocomposites with different filler contents	70

No.	Title	Page
(4-8)	Average crystallite size and microstrain of the PVDF/$Ba_{0.6}Sr_{0.4}TiO_3$ nanocomposites with different filler contents	73
(4-9)	(XRD) data of PVDF/$Ba_{0.7}Sr_{0.3}TiO_3$ nanocomposites with different filler contents.	76
(4-10)	Average crystallite size and microstrain of the PVDF/$Ba_{0.7}Sr_{0.3}TiO_3$ nanocomposites with different filler contents	78
(4-11)	Surface roughness, root mean square (RMS) roughness and grain size of $Ba_{0.6}Sr_{0.4}TiO_3$ and $Ba_{0.7}Sr_{0.3}TiO_3$ nanopowders	79
(4-12)	The optical energy gap for allowed direct transition of (PVDF/BST6) nanocomposites with different filler contents	106
(4-13)	The optical energy gap for allowed direct transition of (PVDF/BST7) nanocomposites with different filler contents	110
(4-14)	The optical energy gap for allowed direct transition of (PVDF/BST6) nanocomposites with different filler contents unirradiated and irradiated with doses (4.32 kGy) and (4.98 kGy)	115
(4-15)	The optical energy gap for allowed direct transition of (PVDF/BST7) nanocomposites with different filler contents unirradiated and irradiated with doses (4.32 kGy) and (4.98 kGy)	121

List of Symbols and Abbreviations

Symbol	Definition	unit
f	Frequency	Hz
ε´	Dielectric constant	--
tan δ	Tangent loss angle	--
n	Order of reflection	--
θ	Bragg's angle	degree
λ	Wavelength	Å
d_{hkl}	Spacing between diffraction planes.	Å
a_o	Lattice constant	Å
c_o	Lattice constant	Å
hkl	Miller indices	--
D	Average crystallite size	nm
β	Full Width at Half Maximum (FWHM)	Radians
S	Microstrain.	--
d	Separated distance	mm
C_o	Vacuum capacitance	F
C	Capacitance of dielectric material	F
ε_o	Permittivity of free space.	F/m
ε	Permittivity of the dielectric material	F/m
P_w	Loss of power	W
V	Voltage	V
R	Resistance	Ω
I	Current	A
X_c	Impedance of capacitor	Ω

Symbol	Definition	unit
ω	Angular frequency ($\omega=2\pi f$)	Radians/s
φ	Phase angle	degree
ε''	Imaginary dielectric constant	--
I_a	Active current (resistive current)	A
I_r	Reactive current (capacitive current)	**A**
Q	The quality factor	--
σ_{ac}	ac conductivity	$(\Omega.m)^{-1}$
T	Transmittance	--
A	Absorbance	--
α	Absorption coefficient	cm^{-1}
t	Thickness of the sample	cm
E_v	Valence band energy	eV
E_c	Conduction band energy	eV
E_g	Band gap energy	eV
$h\upsilon$	Photon energy	eV
k	Wave vector	cm^{-1}
k_e	Electron wave vector	cm^{-1}
k_{ph}	Photon wave vector	cm^{-1}
k_i	Initial wave vectors of transited electron	cm^{-1}
k_f	Final wave vectors of transited electron	cm^{-1}
A, B	Constants depending on properties of conduction and valance bands	--
D	Charge density	C/m^3
d	Piezoelectric coefficient	C/N
E	Electric field	V/m
T	Stress	Pa
s	Compliance	1/Pa

Symbol	Definition	unit
PVDF	Poly(vinylidene fluoride)	--
BST	Barium strontium titanate	--
BST6	$Ba_{0.6}Sr_{0.4}TiO_3$	--
BST7	$Ba_{0.7}Sr_{0.3}TiO_3$	--
XRD	X-ray diffraction	--
JCPDS	Joint Committee on Powder Diffraction Standards	--
AFM	Atomic force microscopy	--
RMS	Root mean square roughness	--
FESEM	Field-emission scanning electron microscopy	--
SEM	Scanning electron microscope	--
FTIR	Fourier transform infrared spectroscopy	--

Chapter One

Introduction and Previous Studies

1.1 Introduction

In the recent years, material scientists are putting lots of interest for the development of new multifunctional ceramic, polymer and composite materials for many device applications in electronics, optoelectronic industry and biodevices [1,2]. Polymer composites, in general, and ferroelectric polymer-ceramic composites, in particular, have received a significant attention in view of their technological importance in devices such as high energy density capacitors, sensors, actuators, transducers etc. [3]. The fabrication of composites is to combine two or more different materials/phases having different properties to obtain the suitable material properties that often cannot be obtained in single-phase materials [4].

Polymers are inert materials, light weight and generally have a high degree of ductility, which is characterized by low electrical and thermal conductivity so used as insulators, when it is compared with the metals they are low density, large elongation when there is a change in temperature, low stiffness, high resistance to corrosion and they do not consider hardened materials. Ceramic materials are inorganic and non-metal, such as oxides, carbides, etc., where ceramic materials tend to be poor electric and thermal conductivity, , this is means insulating material characterized by brittle resulting from decrease of ductile and thus lower resistance to shocks, but it has the hardness and compression strength and chemically lethargic, Thus ceramic is not used in applications under the effect of impact loads compared to metals, however, it is resistant to high temperatures [5-7].

Nanotechnology is now recognized as one of the most promising technologies. Among various materials research, piezoelectric polymer nanocomposites is emerging as a multidisciplinary research activity and favorable materials for variety medical and electrical applications. One of most important of the piezoelectric polymer is poly(venyliden fluoride) PVDF [8].

Polymer nanocomposites, a multiphase solid material where one of the phases is less than (100 nm) size, are becoming popular and being manufactured commercially for various diverse applications, various types of nanomaterials with various shapes and sizes are being used to prepare polymer nanocomposites. The nanofillers can be in the form of nanoparticles (e.g. carbon, metal powder), nanoplateletes (e.g. silicates), nanowires (e.g. carbon nanotubes, ceramic nanowires) etc. [9]. Polymer composites are important commercial materials with applications that include filled elastomers for damping, electrical insulators, thermal conductors, and high-performance composites for use in aircraft, and from important applications as nanoscale are sensors, electronic and optical nanodevices [10].

1.2 Polymer composites

Polymer composites are commonly defined as heterogeneous system of polymers containing inorganic or organic filler in various forms with either micro or nano in size. The fillers are embedded into polymer to form material which consists of two or more components. This causes modifying of properties for individual component which provides opportunity to prepare new application and commercial value [11].

The polymer composites are attractive materials and they have been intensively studied due to light weight, ease of processability and excellent properties. In fact, there are several reasons to apply fillers and reinforcements into the viscoelastic polymer materials. Firstly, incorporation of filler into polymer in order to upgrade product performance, including physical properties (i.e., conductivity, dielectric constant and density), mechanical properties (i.e., strength and modulus), rheological properties (i.e., viscosity and viscoelasticity). Polymer composites are widely used in several applications such as automotive, tires, packaging and electronic products [12,13].

Incorporation of filler in polymer has been achieved and studied in the past for reinforcing polymer and elastomer. A variety of theoretical and experimental studies have been reported on the reinforcement effect in terms of macroscopic mechanical properties [14]. For example, reinforcement effect of carbon black and silica, the most commonly used reinforcing fillers, led to the development of many high engineering performance products for elastomers and plastic industries [12,15]. Secondly, fillers are used for economic reason which is to reduce the cost of production [13].

Nowadays, there has been an increasing interest in the preparation of polymer composites for electronic applications with high dielectric permittivity. These composites offer high and predictable dielectric permittivity, low dielectric loss, mechanical flexibility as well as easy fabrication [14, 16]. Generally, polymers are materials with low dielectric permittivity ($\varepsilon' = 2$ to 10) [16], as summarized in Table (1-1). They do not

meet the application requirements of high capacity, especially non polar polymer which has no permanent dipole moments. The improvement in dielectric permittivity of polymer can be obtained by mixing the insulating polymer with high permittivity ceramics fillers (ε′=1000 to 2000) and very low loss factor (i.e., Barium Titanate (BT) [17], Bismuth Sodium Barium Titanate [18] and Lead Zirconate Titanate (PZT)) [19] etc. Another approach to increase permittivity of polymer is to utilize conductive fillers such as carbon black, metal particle and carbon nanotube. However, this approach gets very high dielectric loss because the filler particles can easily form a conductive path in the composite [20].

Table (1-1): Dielectric constant (ε′) and loss tangent (tanδ) of some polymers [21].

Polymer	Frequency	ε′	tan δ
Poly(vinylidene fluoride) PVDF	1 kHz	10.5	0.026
Poly(vinylidene fluoride-co-trifluoro ethylene)	1 kHz	11	0.184
Polyethylene (PE)	1 MHz	2.3	0.0001
Epoxy	----	4.2	0.0082
Nylon-6 (PA6)	1 kHz	8	0.1
Natural rubber (NR)	1 kHz	2.7	0.002
Ethylene propylene rubber (EPR)	1 kHz	3.2	0.0066
Chloroprene rubber (CR)	1 kHz	6.5	0.03
Polyurethane (PU)	1 kHz	5	0.015

Nowadays, polymer-ceramic composites have been developed to improve dielectric permittivity of the individual polymers because they generally suffer from low dielectric permittivity. However, they are easily processed with high ability to stretch [14,16]. These types of composites are possible to combine desirable characteristics such as mechanical flexibility, chemical stability and processing possibilities of the polymer and the high dielectric constant (permittivity), piezoelectricity and stiffness of ceramics [22].

1.3 Piezoelectric Materials

Piezoelectric materials are a class of materials that can transfer mechanical energy to electrical energy and vice versa. The piezoelectric effect consists of a linear coupling between an applied electric field and an induced strain. In other words, an input of mechanical energy will produce an electrical polarization. The reverse phenomenon also occurs; applying an electrical polarization will cause changes in dimensions. The response of the material is proportional to the electric field or change in dimension. This predictable material property is extremely valuable in sensing and actuation [23,24].

Pierre and Jacques Curie discovered the piezoelectric effect in the late (1800's) when they realized that certain materials deform when an electric potential is placed across them. The importance of such materials was quickly realized and it was soon found that quartz crystals could vibrate at various frequencies by applying electromagnetic radiation. By World War II, the U.S. Army used quartz crystals to send messages over radio waves. Since then, many different materials have been investigated for their piezoelectric response. Naturally occurring crystals and other materials such as quartz, bone and wood were among the first to be evaluated. Synthetic materials are

perhaps the most well known because they exhibit the largest measurable responses to electric fields. Ceramics like Barium Titanate ($BaTiO_3$) and Lead Zirconate Titanate (PZT) are some of the most popular materials currently used in industry [25,26].

Piezoelectric materials are part of a class of materials called ferroelectrics. Ferroelectric materials are substances that have an electric polarization reversible by an electric field. All piezoelectric materials are ferroelectric in that they are naturally polarized or polarizable when exposed to specific conditions. However, not all ferroelectrics exhibit the same ability to produce an electric potential when deformed as do peizoelectrics. Ferroelectrics may also exhibit pyroelectric behavior, where a net change in potential occurs with changes in temperature [26,27].

The response found in piezoelectrics occurs in few materials and depends greatly on the material's molecular arrangement. Piezoelectricity is a third-rank tensor property that is found only in acentric materials. Most of these materials are crystalline and their molecular structure allows the individual crystals within the material to act collectively producing a measurable net response. When these crystals are not oriented, there is no net response. Almost all materials are electrostrictive, in that they expand or contract in the presence of an electric field. The response of electrostrictive materials is very small and acts in all directions. Piezoelectrics only respond in one or two directions due to their asymmetric nature, and the response is useful in actuator and sensor applications. The small electrostrictive material response is not as useful as the piezoelectric response but stronger electrostrictive responses can influence material properties [26,28].

1.4 Piezoelectric Polymers

Polymers are researched extensively as piezoelectric because of their unique properties and advantages over other piezoelectric properties. The piezoelectric response of polymers is less pronounced than those of single crystal inorganics, but polymers do have their advantages. Poly(vinylidene fluoride), in particular, has high chemical resistance, and high efficiency in converting mechanical energy to electrical. Polymers are easier to manufacture, often at lower temperatures, and can be formed more easily into custom shapes for use in complex operations. In addition, polymers are inherently flexible, have relatively low modulus and low mechanical impedance, with high sensitivity to mechanical loads. These properties make them more versatile than other piezoelectric materials for sensing and actuation. There are a few other semicrystalline organic materials that show piezoelectric properties, but none have shown as same magnitude of response of poly(vinylidene fluoride) and its copolymers [29-31].

Heiji Kawai discovered the piezoelectric properties of (PVDF), in (1969). Furakawa and Johnson confirmed (PVDF's) piezoelectric nature in 1981 and identified the Curie point of (103ºC). (The Curie point is the temperature above, which the piezoelectric effect breaks down.) Before (1969) the only materials that received much attention for their ferroelectric or piezoelectric properties were naturally occurring crystals, such as quartz, and man-made ceramics, such as Barium Titanate and Lead Zirconate Titanate [25,27].

Piezoelectric polymers are much more sensitive in responding to deformations and electric fields than ceramics and are much more durable [26].

1.4.1 Applications of Piezoelectric Polymers

Piezoelectrics have been used to sense forces, deformation, and changes in temperatures. These devices have been incorporated into systems where the data they collect are used to control how they respond to their environment. There are forms that can directly or indirectly control their response to environmental changes and are now being incorporated in smart structures. Smart structures incorporate actuators, electromagnets, controllable fluids, etc, to adjust to their surroundings. The main advantages with piezoelectric materials in smart structures are that they sense micrometer level displacements at high frequencies and use little power for actuation [23,28].

Piezoelectric polymers are extremely useful in monitoring vibrations and in controlling flexible structures. Not only can they be used to measure the extent of deflection and frequencies of vibration, they can also control the structure through actuation. Piezoelectrics in general can be bonded to surfaces or can be embedded within structures. Using multiple layers of (PVDF), one of its copolymers, or another piezoelectric polymer, it is possible to sense the vibrations in one layer and control the vibration with another [26].

1.5 Poly(vinylidene fluoride) (PVDF)

Poly(vinylidene fluoride), or poly(1,1-difluoroethylene) is known by its acronym\PVDF. The structure of (PVDF) is presented in Figure (1-1). (PVDF) is prepared in aqueous medium by polymerization of vinylidene fluoride (CH_2=CF_2). Polymerization procedures, temperatures, pressure, recipe ingredients, monomer feeding strategy, and post polymerization are variables influencing product characteristics and quality [32,33].

Addition of monomeric units in a 'head-to-head' or 'tail-to-tail' defects is out of control during the polymerization which is caused by temperature of polymerization. The defect structure around (3-6) % affects the crystallinity and mechanical properties of (PVDF) [34].

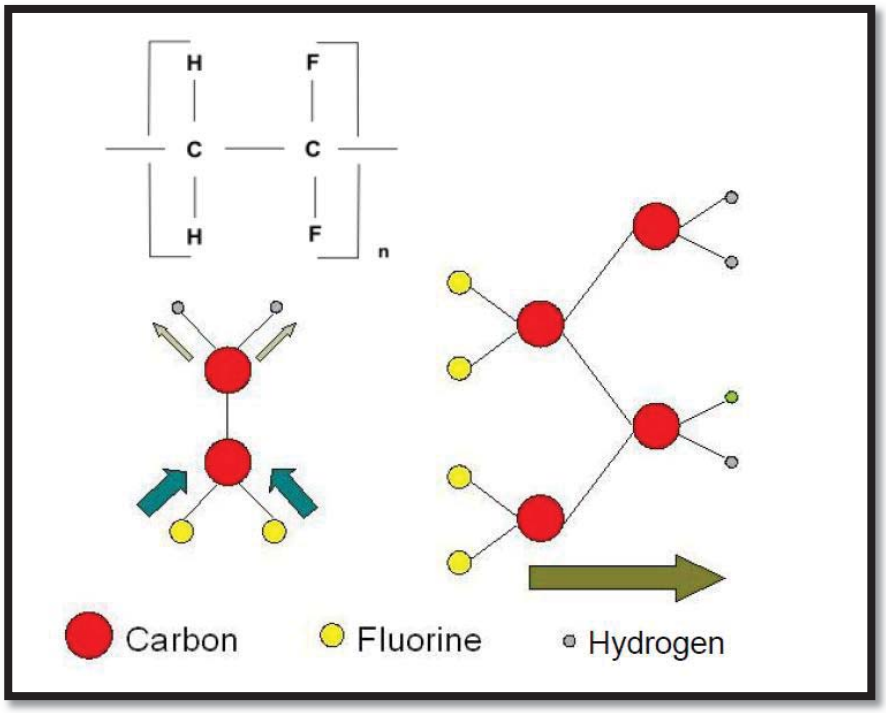

Figure (1-1): Structure of (PVDF) [21].

(PVDF) is typically a semicrystalline polymer that is approximately (50%) amorphous. The structure of the monomer is -CH_2-CF_2-, and the chains occur mostly in a head to tail configuration. The molecular weight of (PVDF) is typically between (60) and (70) kg/mol [35].

As with most polymers, the mechanical, rheological, and electrical properties of (PVDF) have been extensively studied. Most investigations focus on two properties of particular importance. The first is the polymer's polymorphism, and second is (PVDF's) piezoelectric properties. (PVDF's) ferroelectric properties are what make this polymer so unique. (PVDF) is

considered to have a stronger piezoelectric response compared with other polymers and is considered easy to process into films [26,36].

Other than its piezoelectric properties, poly(vinylidene fluoride) is a useful polymer due to its chemical stability, resistance to organic solvents, and high elastic modulus compared with other polymers. (PVDF) has shown to be very useful as a dielectric because of its high permittivity and dielectric strength and low dissipation factor. Compared to other polymers and other piezoelectric materials in general, (PVDF) has many benefits; some of its more important properties are listed below [26,36,37]:

- High rigidity, resists deformation.
- Low glass transition temperature (no transitions between (–45°C) and (170 °C).
- Wide range of processing temperatures (185 – 250) °C.
- Resistance to heat and combustion.
- Resistance to ageing.
- Resistance to abrasion.
- Chemically inert.
- Non toxic.
- Chemically resistant (highly polar solvents will cause slight swelling).
- Excellent electrical insulator.
- High Curie point (103 °C, valuable for high temp piezoelectric applications).

(PVDF) has four known crystalline structures, referred to as (α, β, γ and δ) phases. The α-phase is the common polymorph of (PVDF) and is normally obtained by crystallization from the melt at moderate or high under cooling. The α-phase consists of a series of non-polar anti-parallel packing of chains. The β-phase is currently the most important of (PVDF) polymorph being used extensively in piezoelectric application. β-phase consists of a series of polar parallel chains [38]. Figure (1-2) shows the chain formation for the α, β and γ-phases of (PVDF).

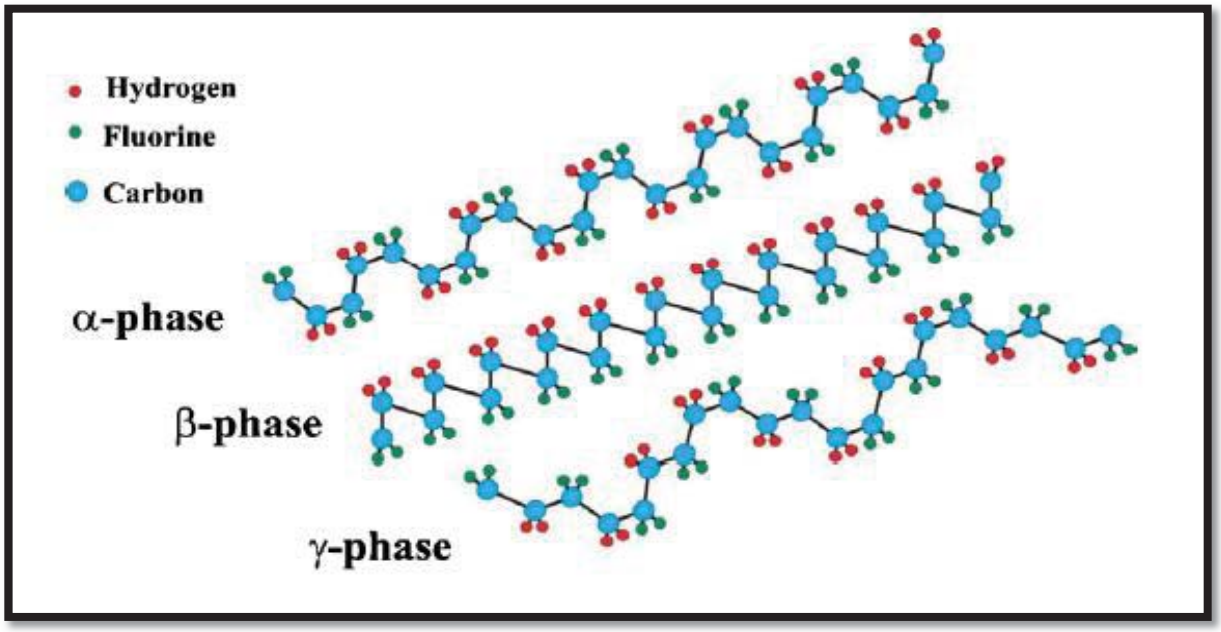

Figure (1-2): Schematic representation of the chain formation for the α, β and γ-phases of (PVDF) [39].

(PVDF) and its copolymer have been extensively used for composites and blend because of its potential applications to high dielectric permittivity, and unique piezoelectric, and ferroelectric properties. As mentioned above, a lot of investigations have been focused on the development of polymer/ceramics composites by using ferroelectric ceramics as fillers in (PVDF) to increase dielectric permittivity of composite [40,41].

1.6 Ferroelectric Perovskite Materials

As one of the most important materials for both fundamental science and technical applications in electronic industry, ferroelectric perovskite materials have attracted tremendous attention. Industrial applications of these materials embrace embedded capacitors, multilayered ceramic capacitors (MLCCs), transducers, sensors, memory, and power storage devices. With the ever-growing trend towards integration, miniaturization and versatility, ferroelectrics at nanoscale regime have been thoroughly studied through chemical synthesis, experimental physics, computer modeling, material property analysis, etc. [42,43].

Possessing a spontaneous dipole moment, the orientation of the polarization of ferroelectric materials can be switched by the application of an electric field. The ferroelectricity of perovskite materials occurs in the tetragonal phase, where the center atom moves off-center due to the change of the external field, leaving a (180°) difference in polarization direction. Materials falling into this category include: $BaZrO_3$, $PbTiO_3$, $PbZrO_3$, $(Ba,Sr)TiO_3$, $Pb(Zr,Ti)O_3$, $LiNbO_3$, etc. [43,44].

1.7 Barium Strontium Titanate (BST)

Barium Strontium Titanate (BST, $Ba_xSr_{(1-x)}TiO_3$) is one of the most attractive materials which are currently being studied for a variety of applications such as tunable microwave components, humidity and gas sensors, pyroelectric and wireless temperature sensors or as dielectric layers in electroluminescent display devices [45]. (BST) is a solid solution of Barium Titanate (BTO, $BaTiO_3$) and Strontium Titanate (STO, $SrTiO_3$) and thereby inherits properties from both its parents. Barium Titanate has a perovskite

tetragonal crystalline structure and Strontium Titanate has a perovskite cubic structure at room temperature. Strontium atoms displace the Barium atoms, changing the crystal structure and properties. (BST) has an ABO_3 perovskite structure, and its high dielectric constant is due to ionic displacements from a centro-symmetric structure [46,47].

(BTO) has a Curie temperature of (395 K), while (STO) has a Curie temperature of (20 K). The Curie temperature, (T_c), is a transition temperature. A material is in its paraelectric phase at temperatures above (T_c), and is in its ferroelectric phase at temperatures below (T_c). In the ferroelectric phase, atoms shift away from their position and the crystal symmetry changes. This is depicted in Figure (1-3). Hence, the transition temperature of (BST) will lie in between the two extremes, depending on the ratio of Barium to Strontium. The dielectric constants of the ceramics are the highest at the Curie temperature. From Figure (1-4), it can be seen that (T_c) decreases linearly with an increased concentration of Strontium [48].

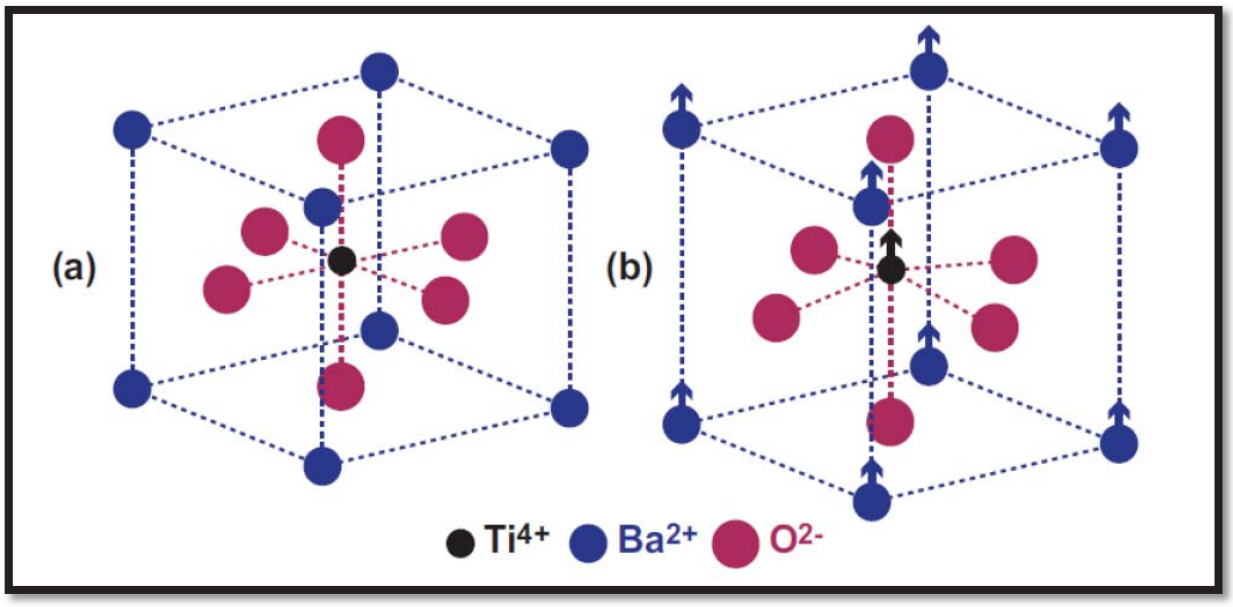

Figure (1-3): (a) Paraelectric phase (centro-symmetric) (b) Ferroelectric phase (displaced) of (BST) [47].

The Curie temperature of (BST) ($Ba_xSr_{(1-x)}TiO_3$) is closest to room temperature when (x = 0.7), and therefore, the relative permittivity is at a maximum. Overall, Barium Titanate can achieve the highest dielectric constant, but only at its (T_c), which is at (120°C). The permittivity is lowered at (25°C) [48].

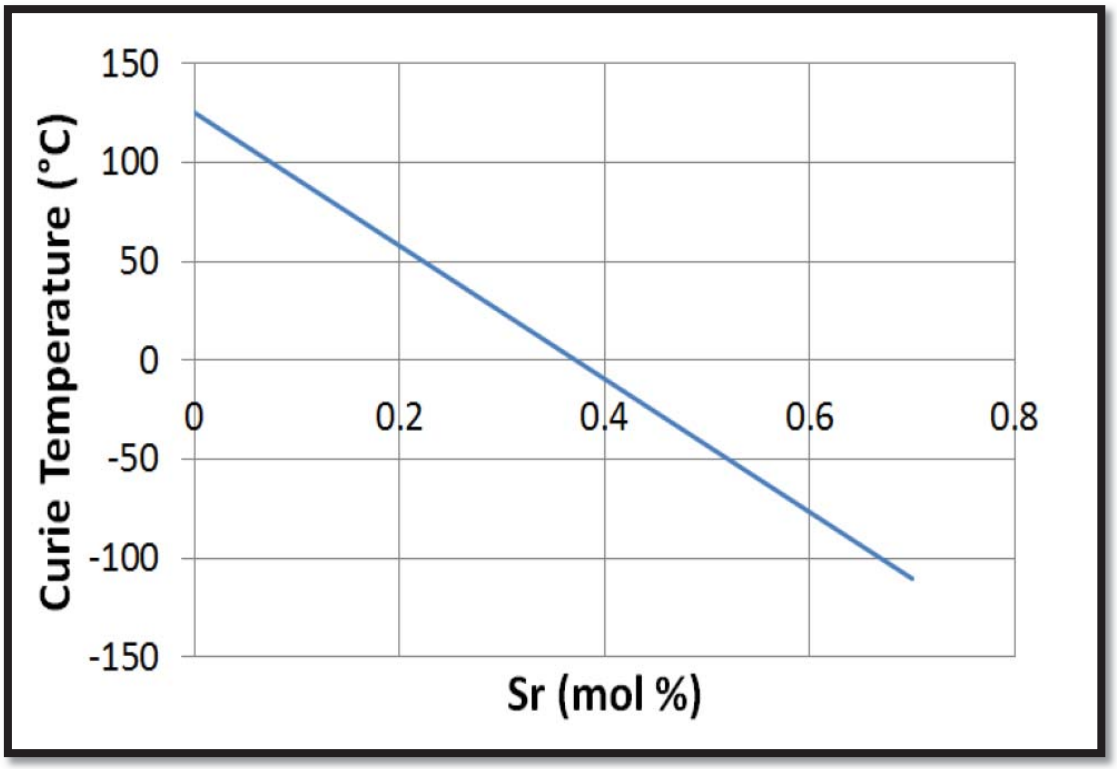

Figure (1-4): BST Curie temperature is linearly dependent on concentration of Sr [48].

1.8 Previous Studies

Tian *et al.* (2001) studied the optical properties of amorphous and polycrystalline $Ba_xSr_{1-x}TiO_3$ (BST) films fabricated by a sol–gel spin-coating technique. It is found that the band gap energy of the films decreases from (4.15) to (3.75) eV with increasing Ba/Sr ratio from (0.7) to (1.0) [49].

Razak *et al.* (2006) produced Barium Strontium Titanate (BST) in a teflon lined pressure vessel using a high temperature hydrothermal technique and controlling the processing parameters of Ba+Sr concentration, Ba and Sr ratio, temperature, reaction period and TiO_2 concentration. It was found that this technique produces BST powders of less than (200 nm) particle size with high degree of crystallinity. The dielectric constant at room temperature increased when the amount of TiO_2 increased in the reaction. A similar trend is observed for samples with (Ba:Sr) ratios. The highest value of dielectric constant was observed for the Ba richest sample [50].

Razak *et al.* (2007) produced Barium Strontium Titanate (BST) in a pressure vessel at (220 °C) using the hydrothermal technique. Ba and Sr concentrations, temperature, reaction time and Ti concentration were varied to study the effects of processing on the formation of (BST). Structure of the final (BST) product was greatly affected by two major parameters: Ba:Sr mol ratio and TiO_2 concentration. As Ba and Sr have different chemical activity and mobility, they react differently with Ti, leading to a multi-phase structure in the case of a small deficiency in Ti, and a single phase for a high deficiency in Ti. The threshold value of (Ba + Sr)/TiO_2 ratio for a single/two phase

transition was about (3). The obtained phases were tetragonal $BaTiO_3$ and cubic $Ba_{0.6}Sr_{0.4}TiO_3$, if a relative share of Sr was small, less than (10%). As the amount of Sr increases it goes mostly to the cubic structure. When Sr concentration in the initial solution reaches (30%), the final (BST) becomes three phase. This process is also accompanied by Ba losses. For every introduced percent of Sr there is a (1.6%) of Ba loss [51].

Fu *et al.* (2008) prepared $Ba_{0.6}Sr_{0.4}TiO_3$ (BST40) nano powders by a low temperature hydrothermal process. (XRD) patterns showed that a cubic perovskite structure could be synthesized and SEM certified that the size of powders was about (80 nm). Temperature dependence of dielectric constant and tan δ were measured in the range of (30 °C) to (500 °C) at frequencies from (1 kHz) to (1MHz) for ceramics sintered at (1200 °C) and (1350 °C) [52].

Miao *et al.* (2008) studied microstructure and dielectric properties of the nanosized $Ba_xSr_{1-x}TiO_3$ powders of different compositions synthesized by hydrothermal method. The result showed that perovskite structure of the (BST) powders was developed through the mutual diffusion between the intermediate phase and TiO_2 phase. The (BST) powders were well developed and tetragonal crystals were observed. The grain size of the $Ba_{0.77}Sr_{0.23}TiO_3$ (BST77) powders ranged from (20) to (40) nm. Maximum dielectric constant was achieved at the testing temperature of (5.7 °C) and the (BST) ceramics with large grain size showed large dielectric constant [53].

Li *et al.* (2009) prepared nanocomposite by the silver mirror reaction by embedding $Ba_{0.6}Sr_{0.4}TiO_3$ (BST)/Silver core/shell nanoparticles (BST-Ag) into polyvinylidene-fluoride (PVDF). Through functionalizing the surface of BST nanoparticles by silver coating, the relative permittivity of composites was significantly increased to (153) at (100 Hz) which is (73%) higher than that of the composite making of untreated (BST) nanoparticals. The loss tangent was still low less than (0.2) when the filler content of (BST-Ag) was (0.55) [54].

Song *et al.* (2012) prepared $Ba_{0.6}Sr_{0.4}TiO_3$ (BST) nanofibers via electrospinning and modified by dopamine are used as dielectric fillers in polyvinylidene fluoride (PVDF)-based composites. It was found that the dielectric constants of the (BST/PVDF) composites increases from (8) to (23) with (BST) fillers increasing from (0 vol%) to (11.2 vol%). The dielectric loss of the (BST/PVDF) composites increases with the increasing of frequency [55].

Yu *et al.* (2013) have prepared ceramics-polymer nanocomposites consisting of surface treated $BaTiO_3$ (BT) particles as fillers and poly(vinylidene fluoride) (PVDF) polymer as matrix by using a solution casting process. It is found that the dielectric permittivity of the nanocomposites increases steadily as (BT) content increases over the whole frequency range from (10^3) to (5×10^7) Hz. The loss tangent exhibits little variation in the frequency range from (10^3) to (10^5) Hz and then increases to a sharp peak around (4×10^7 Hz) which is attributed to the glass transition relaxation of the (PVDF) [56].

al Indolia *et al.* (2013) studied the optical properties of (PVDF-ZnO) nanocomposite films prepared by solution casting method. It is found that the direct band gap of (PVDF) film is (5.66 eV) and the indirect band gap is (4.96 eV), The optical band gap for direct and indirect transitions for this system decreases as the ZnO content increases. This behavior may be associated with the structural changes occurring after addition of ZnO nanoparticles [57].

Zhou *et al.* (2013) prepared Barium Strontium Titanate ($Ba_xSr_{1-x}TiO_3$) (BST) films by a two-step hydrothermal reaction and without the need for costly equipment. The dielectric constant and ferroelectric properties of the film can be tuned by varying the (Ba:Sr) molar ratio of the materials. It was found that the dielectric constant of the (BST) film varying from (300) to (800) as the Curie temperature decreases with increasing volume fraction of $SrTiO_3$ in the solid solution. The maximum dielectric constant reaches (811) when the molar fraction of barium is (0.71) [58].

Liu *et al.* (2014) prepared ceramic−polymer nanocomposites consisting of $Ba_{0.6}Sr_{0.4}TiO_3$ nanofibers (BST NF) with a large aspect ratio via electrospinning and employing surface hydroxylated as fillers and poly(vinylidene fluoride) (PVDF) as matrix by a solution casting method. The nanocomposites exhibit enhanced permittivity, reduced loss tangents and improved breakdown electric field strength at a low volume fraction of hydroxylated (BST NF). The relative permittivity of the nanocomposites increases with the content of the (BST NF−OH) and reaches up to (25) at (10 vol%) (BST NF−OH). And the relative permittivity of the (BST NF−OH/PVDF) is bigger than that of the (BST NF/PVDF). The loss of the (BST NF−OH/PVDF) is lower than that of the (BST NF/PVDF) [59].

Liu *et al.* (2014) studied the dielectric properties of surface-hydroxylated $Ba_{0.6}Sr_{0.4}TiO_3$ nanotubes (BST NT) filled poly(vinylidene fluoride) (PVDF) composite films prepared by a solution casting method. The dielectric constant of the composites gradually increases with the content of BST NT-OH within a wide range from (2.5 vol%) to (10 vol%). The maximum dielectric constant is (48.2) at (1 kHz) with (10 vol%) (BST NT-OH), which is (6.1) times higher than that of the pure (PVDF) (7.9) [60].

Liu *et al.* (2015) prepared surface-modified $Ba_{0.6}Sr_{0.4}TiO_3$ nanofiber (BST NF)/poly(vinylidene fluoride) (PVDF) nanocomposites by solution casting method. Surface modification of dielectric fillers was obtained through functionalization of the (BST NF) by hydroxylation using H_2O_2 treatment and subsequent fluorination. Surface fluorination could facilitate the homogeneous dispersion of the nanofiber fillers in the (PVDF) polymer matrix. The enhanced dielectric constant, reduced loss tangents and improved breakdown strength were obtained in (PVDF-based) nanocomposites filled with (F-BST NF). The dielectric constant of the composites gradually increases with the content of (F-BST NF) within a wide range from (2.5 vol%) to (7.5 vol%), which means it can be tuned by changing the (F-BST NF) content. The maximum dielectric constant is (22.5) at (7.5 vol%) (F-BST NF), which is (2.84) times higher than that of the pure (PVDF). Compared with the (BST NF/PVDF), the (F-BST NF/PVDF) nanocomposite films with the same filller content not only shows a higher dielectric constant but also has a lower dielectric loss at a frequency of (1 kHz) [61].

Hu *et al.* (2015) prepared poly(vinylidene fluoride) (PVDF) / barium strontium titanate (BST) composites by solution casting method. The microstructure and dielectric properties of composites comprising polyvinylidene fluoride (PVDF) and Barium Strontium Titanate (BST) particles have been investigated. The SEM of the composites revealed the excellent distribution of (BST) fillers in (PVDF) matrix. It was found that the permittivity of the (BST/PVDF) composites increases from (16) to (40) while loss tangent decreases from (0.27) to (0.19) with (BST) fillers increasing from (10 vol%) to (40 vol%). The permittivity and loss tangent of the (BST/PVDF) composites decreases with the increasing of frequency (10^2–10^6) Hz [62].

Zhang *et al.* (2016) prepared $(Ba_{0.6}Sr_{0.4})TiO_3$ (BST)/ poly(vinylidene fluoride) (PVDF) composites by tape casting using aminopropyl triethoxy silane (KH550) modified (BST) particles and (PVDF) matrix polymer. It is found that the dielectric constant increases slowly with the increase of content of (BST) fillers, meanwhile, the dielectric constant of composites modified with (KH550) was higher than that of unmodified (BST/PVDF) composites at the same composition, while the loss tangent exhibits a trend opposite to that of the dielectric constant. For composites the surface modification of (KH550) led to an increase of the permittivity with (10 – 40) vol% (BST), from about (16, 19, 29, 40) at (1 kHz), for composites made with unmodified respectively, to about (20, 26, 40, 56) at (1 kHz) for the modified powders. The loss tangent decreases from (0.27, 0.16, 0.17, 0.22) to (0.18, 0.15, 0.13, 0.18), respectively. The results again certify that the composites with (4 wt%) (KH550) exhibit a better dielectric performance than the other composites with the same content of (BST), which have higher dielectric constant and lower dielectric loss than other samples [63].

Liu *et al.* (2016) studied the dielectric properties of poly(vinylidenefluoride) (PVDF) nanocomposites with $Ba_{0.6}Sr_{0.4}TiO_3$ nanoparticles (BST–NPs) fillers. The (BST–NPs) were synthesized by using a molten salt method. (BST/PVDF) nanocomposites were fabricated by using a solution casting method. The nanocomposites exhibited increased dielectric constant and improved breakdown strength. Dielectric constants of the nanocomposite with surface hydroxylated (BST–NPs) (BST–NPs–OH) were higher as compared with those of their untreated (BST–NPs) composites. The sample with (40 vol %) (BST–NPs–OH) had a dielectric constant of (36) at (1 kHz) and pure (PVDF) had a low dielectric constant of (7.9). The dielectric constant gradually increases with the increasing of filler content [64].

Pereira *et al.* (2016) studied the degradation of (PVDF) polymer exposed to Gamma irradiation in Oxygen atmosphere in high dose rate and compared to degradation of (PVDF/Graphene Oxide) (PVDF/OG) composites prepared using a solution method. The samples were irradiated with a Co-60 source at with doses ranging from (100 kGy) to (1,000 kGy). In (FTIR) data shown that the formation of oxidation products was at the both samples with formation of carbonyl and hydroxyl groups amongst the most prevalent products in the pure (PVDF) samples. In the other hand, the composites samples exhibit less presence of degradation products with predominant formation of carbonyl groups, these results also seen in the (UV-Vis) analysis. The absorbance of pure (PVDF) polymer and (PVDF/OG) composite increased with the increasing of irradiation doses. The results show that the samples of composites may have greater resistance to the irradiation process, since they have less degradation products than pure (PVDF) samples seen by spectroscopic techniques [65].

Pan *et al.* (2016) studied Microstructure and dielectric properties of a composite material based on surface functionalized $Ba_{0.6}Sr_{0.4}TiO_3$ nanofibers/poly(vinylidene fluoride) (BST NF/PVDF) prepared by solution casting method. The nanocomposites containing (7.5 vol%) isopropyl dioleic(dioctylphosphate) titanate (NDZ101) functionalized (BST NF) (N-h-BSTNF) have maximum dielectric permittivity of (20.56) at (1kHz) which is (2.49) times higher than that of the pure (PVDF) (8.26) at (1kHz) [66].

Wang *et al.* (2016) studied the effect of the (BST) nanoparticle contents on the microstructure and dielectric properties of $Ba_{0.6}Sr_{0.4}TiO_3$ (BST)/poly(vinylidene fluoride) (PVDF) nanocomposites. (BST/PVDF) nanocomposites with (BST) nanoparticle contents of (10–40) vol% were prepared by tape casting method. The (BST) nanoparticles with (~60 nm) crystal size were obtained by sol–gel method. The (SEM) images of (BST/PVDF) nanocomposites with different contents of (BST) nanoparticles certify that the incompatibility between the (BST) nanoparticles and the (PVDF) matrix becomes more and more obvious with increasing volume fractions of the nanoparticles. The dielectric constant and loss tangent of the nanocomposites increased from (14.1) to (29.7) and (0.069) to (0.21) at (1 kHz) and room temperature, with the increasing of (BST) nanoparticles contents [67].

Revathi *et al.* (2018) synthesized nanostructured $PbZr_{0.52}TiO_{0.48}O_3$ (PZT) powder at (500–800) °C using sol–gel route. (XRD) confirmed the formation of perovskite structure. The (PZT) powder and (PVDF) were used to form the (PZT/PVDF) composite film using solvent casting method. The composite films containing (10%, 50%, 70% and 80%) volume fraction of

(PZT) in (PVDF) were fabricated. The (XRD) spectra validated that the (PZT) structure remains unaltered in the composites and was not affected by the presence of (PVDF). The (SEM) images show good degree of dispersion of (PZT) in (PVDF) matrix and the formation of pores at higher (PZT) loading. The optical band gap of the (PVDF) film is (3.3 eV) and the optical band gap decreased with increase in volume fraction of (PZT) fillers. The (FTIR) spectra showed the bands corresponding to different phases of (PVDF) (α, β, γ) and perovskite phase of (PZT). The dielectric constant was measured at frequency ranging from (1 Hz) to (6 MHz) and for temperature ranging from room temperature to (150 °C). The composite with (50%) (PZT) filler loading shows the maximum dielectric constant at the studied frequency and temperature range with flexibility [68].

Hu *et al.* (2018) prepared (BST) ceramic nanofibers by the electrospinning method and incorporated into (PVDF) homopolymer after they were treated by H_2O_2. Because of the high dielectric properties and flexoelectric response of the (BST) nanofibers, both dielectric properties and flexoelectric coefficient of the (PVDF/BST) nanocomposites were enhanced by (3–4) times after (25 vol%) nanofibers were added to the (PVDF) polymer. The composites with non-modified fibers were also prepared. Compared with the composites with modified fibers, composites with non-modified fibers may exhibit a slightly higher dielectric constant, but a high dielectric loss and conduction [69].

1.9 Aims of the Study

Polymer-ceramic nanocomposites have received a significant attention in view of their technological importance in devices. In this research project, it has been concentrated on the preparation of nanocomposite from a ($Ba_xSr_{1-x}TiO_3$) (x = 0.6, 0.7) perovskite ceramic powder suspended in a PVDF polymer matrix, and studying the structural, dielectric, optical and piezoelectric properties.